



Antibacterial Activity of Cobalt and Titanium (Co:TiO₂) Core-Shell Nanoparticles against *E. coli* Isolated From Urinary Tract Infections

Usama R. Hameed¹, Laith A. Yaaqoob¹

¹Department of Biology, College of Science, University of Baghdad

Received: 1/6/2022 Accepted: 11/9/2022 Published: December 20, 2022

Abstract: This study aimed to use pyocyanin pigment produced by the clinical isolate *Pseudomonas aeruginosa* as a reducing and stabilizing agent for core-shell nanoparticles of cobalt and titanium (Co:TiO₂) and their antibacterial effectiveness against biofilm-forming, multidrug-resistant *E. coli* obtained from urinary tract infection. (Co:TiO₂) NPs The preparation was in two phases, The first stage is the preparation of Cobalt nanoparticles by using cobaltous chloride hexahydrate (5gm) dispersing in (50ml) of pyocyanin, The second phase adds titanium tetrachloride (1ml) on pyocyanin (150 ml) that contains Cobalt nanoparticles Which were previously prepared. The (Co:TiO₂) NPs synthesized were characterized by various techniques such as UV-VIS, AFM, XRD, FTIR, FE-SEM, and TEM. based on the wavelength of the Cobalt and titanium (Co:TiO₂) core-shell nanoparticles at (284 nm) by spectrophotometer, The diameter was identified by Atomic force microscopy (AFM) the average diameter at 75.48 nm, and the higher concentration of (Co:TiO₂) NPS in the solution at 200 µg/ml It was shown that the maximum inhibitory zones for *E. Coli* were 37 millimeters in diameter. (Co:TiO₂) core-shell nanoparticles have been demonstrated to be effective against *E. Coli* that produce biofilms.

Keywords: Biofilm, pyocyanin, *E. Coli*, core-shell cobalt, titanium nanoparticles (Co:TiO₂ NPs).

Corresponding author: (Email:usama.rasheed1206a@sc.uobaghdad.edu.iq).

Introduction

Nanotechnology is the study of extremely small structures mostly with sizes ranging from (1 to 100 nm), which also provide them with exceptional characteristics when compared to microscopic-sized particles(1). Titanium dioxide nanoparticles (TiO₂NPs) are used in a various range of applications, such as biological, pharmaceutical, environmental purification, electronics, gas sensors, photo-electrodes photo-catalysts, and solar energy cells(2), as well as American Food and Drug Administration (FDA) acceptance for

use in food processing and drugs, cosmetics, ointment and pigment paints. TiO₂NPs can be synthesized by different methods such as biological (18), chemical(9), and physical (17) methods. The process of chemical reduction for titanium dioxide nanoparticle synthesis is still costly and requires dangerous organic solvents and poisonous reducing agents (19). Therefore, Titanium dioxide nanoparticles were created using a biological synthesis approach that is safe, less poisonous, less damaging, and low cost. The use of natural product

extracts is a promising innovation that would resolve the obstacles identified in chemical methods, and the "green synthesis method" is an environmentally friendly system because it uses plant extracts (leaves, flowers, seeds, and peels) rather than large quantities of chemicals for the synthesis of titanium dioxide nanoparticles(11).so far. The secondary metabolite pyocyanin pigment was found to be formed by gram-negative *P.aeruginosa* (6).In spite of their antibacterial capabilities, several heavy metal cations are too toxic to be used in the treatment of infectious disorders. These include Hg^{2+} , Cu^{2+} , and Pb^{2+} . Heavy metals (particularly cobalt) have been the subject of several recent reviews, with experts considering their potential benefits as antibacterial agents and their risks to human cells. Metallic cobalt, as stated in (13), is very hazardous at greater intracellular quantities. It seems that proteins that export or chelate metals are the primary defense mechanisms utilized by live cells to ward against the toxicity of these elements. Cobalt toxicity was studied using a human keratinocyte cell line as a model, and a model was proposed to ascertain the in vitro chemical impact on cell viability of a soluble form of cobalt, even though the biochemical and molecular cobalt-induced toxicological mechanisms are not yet fully identified (Co). These kinds of investigations are now underway, and preliminary findings suggest that reactive oxygen species are responsible for cototoxicity.(5) Cobalt is one of the elements of research interest, applied in the preparation of nanoparticles for biomedical applications. Currently, cobalt oxide

nanoparticles based on cobalt metal can attract more interest from researchers due to their Specific shape, size-dependent characteristics, and also wide applications. (10). The aim of study Antibacterial activity of (CO: TiO_2) core- shell nanoparticles against of *E.coli*.

Materials and methods

Bacterial isolates were collected from a patients suffering from urinary tract infections, from different hospitals, (70%) of them are men and (30%) are women aged between 1-15 years during the period from /December 2021/ to /February 2022/. All bacterial species isolates were identified via conventional biochemical assays. Antibacterial activity and otherwise manufacture of (Co: TiO_2) NPs were investigated using bacterial strains of multi-drug resistance *E. Coli* (14).

Bacterial isolation identification VITEK 2 system

This procedure includes several phases, such as: In the plane test tube, lope-full isolated colony has been introduced into a 3mL of normal saline. An automated density checks confirmed that the colony's concentration complied with McFarland's recommendation of 1.5×10^8 CFU/ml.

Using the barcode on the cassette, computer software could be able to identify the sample when standardized inoculums were added. A sample ID number is associated with the VITEK 2 card type once the barcode has been scanned.

Bacterial isolation identification Biochemical Tests.

Identification by biochemical tests

1- Indole test

Tested bacterial cultures were inoculated with Peptone broth medium and incubated for 18–24 hrs at 37°C. When Kovac's reagent was applied to each tube, the appearance of a crimson ring was regarded as an indication that the experiment had been positive.

2- Catalase production test

A drop of hydrogen peroxide (3 percent H₂O₂) was deposited on a glass slide, and then a loop full of tested bacterial cultures was mixed with hydrogen peroxide; if bubbles appeared, the test was judged positive.

3- Oxidase test

A sterile wooden stick was used to rub a colony of the tested bacterial culture on the oxidase-soaked filter paper. The test was declared a positive if the colony immediately turned ink blue.

4- Motility test

Bacterial cultures were inoculated with Brain Heart Agar media and cultured at 37°C to identify the organisms that moved away from or disappeared into the medium after being stabbed.

5- Urease test

The urea agar slant was incubated at 37°C with a new bacterial culture. The examination results were released after six hrs, twenty-four hours, and six days of testing. Changing the medium's color to purple-pink indicates a experiment had been positive.

6- Simmons Citrate

Bacterial culture was inoculated onto a Simmons citrate slant and incubated at 37°C for 48-72 hours. Positive results are shown by the test results shifting from green to blue.

Testing for antibiotic resistance revealed that *E. Coli* isolates

First, Mueller-Hinton plates need to be prepared.

Mueller-Hinton agar was created using a dehydrated base according to the manufacturer (Himedia/India). Sterilized media placed on the plates, then it was chilled to between 45 and 50 degrees Celsius. Immediately after agar solidification, plates were placed upright in the incubator and dried for 10 to 30 minutes at 35 °C.

The inoculum preparation (Turbidity standard) It was necessary to make inoculums by placing many colonies in a tube containing 5ml of normal saline (NaCl 0.85%), mixing well, and then using the Mcfarland 0.5 turbidity standard to generate culture containing 1.5×10^8 CFU/ml. Suspensions were utilized within 30 minutes of production. Plates inoculated with *E.coli*. A sterile swab was used to culture the inoculums into the plates. When the liquid had been applied, the excess was removed by pushing and rolling the swab firmly on the tube's topmost side and rubbing it three times over the medium's surface at an angle of 60 degrees. A swab was finally used to clean around the borders of an agar plate.

Three, the inoculums were allowed to sit for a few minutes with the lid closed before being tested for bacteria. (Table1). antibiotic that were used for sensitive Antibiotics

Sterile forceps were used to insert the antibiotic disc on the inoculation plate (each plate with 7 to 8 discs). Within 30 minutes, the plates were placed in an inverted position at 37 cc and incubated for 18–24 hours. The findings should be

analyzed. antibiotics that are used for sensitivity.

Table (1): Antibiotics that are used for sensitivity

1	Piperacillin/Tazobactam (PIT) 100\10mg
2	Ertapenem (ETP) 10mg
3	Amoxicillin/clavulanic acid (AMC) 20\10mg
4	Trimethopim\sulphamethoxazol (SXT) 1.25\23.75mg
5	Piperacillin (PRL) 100mg
6	Amikacin (AK) 30mg
7	Imipenem (IPM) 10mg
8	Nitrofurantion (F) 100mg
9	Aztreonam (ATM) 30mg
10	Gentamicin (CN) 10mg
11	Cefotaxime (CTX) 30mg
12	Tobramycin (TOB) 10mg
13	Levofloxacin (LEV) 5mg
14	Meropenem (MEM) 10mg
15	Ceftazidime (CAZ) 30mg

Detection of biofilm (qualitative method)

Detection of the Biofilm formation for isolates of *E. Coli* by using the Congo red agar this procedure includes: The Congo red agar method was used to evaluate *E. Coli* capsule ability to generate biofilm mostly as a presumptive test instead of the formation of biofilm (15). The dye of Congo red agar was employed as a pH indicator in this experiment. Plates that contain Congo red agar media were already seeded and incubated for 24 hours at 37°C in an aerobic environment. Following this time, colonies that have been showing as dark red or blackish and had a dry or quality crystalline were designated, biofilm producers. Biofilm nonproducers were show red colonies with a smooth look.

Detection of biofilm (quantitative method)

After incubating each isolate in 5 ml of Trypticase soy broth (TSB) at

37°C for 18-24 hours (stationary phase), the bacteria were diluted to a final concentration of 0.1 ml/ml and plated in the bottom of polystyrene microtiter plates (180 µl of media+20 µl of bacteria). After incubating at 37 degrees Celsius over the night. Three times, saline containing phosphate buffer was used to wash the cultures in the wells. After 15 minutes of drying at room temperature, the plate was stained with 200 µl of 0.1% crystal violet for 15 minutes. Finally, after 10 to 15 minutes, the wells were filled with 200 µl of 95% ethanol. A microtiter ELISA auto reader optical density readings were taken at 600 nm from the plate wells. They then ran the experiment using sterile TSB as a control. The optical density mean (OD) and the control mean (C) were subtracted from the test (T) values to account for absorbance in the background (4). Biofilm titer may be evaluated in (Table2).

Table (2): Measures the intensity of biofilm for *E. coli*.

Adherence of Biofilm Formation	Interpretation
$OD_s \leq OD_c$	Non-adherent
$OD_c < OD_s \leq 2 * OD_c$	Weakly adherent
$2 * OD_c < OD_s \leq 4 * OD_c$	Moderately adherent
$4 * OD_c < OD_s$	Strongly adherent

Pyocyanin pigment production

Each Sample of *P. aeruginosa* isolate was collected inoculated on Luria-Bertani broth and incubated at 37°C for 72 hrs, According to (7).

Production and extraction of pyocyanin

Using this technique, nutrient agar samples were streaked into Luria-Bertani broth, incubated at 37 C for 120 hours, and then analyzed. After shaking the flask, the pyocyanin green pigment was distributed throughout the entire

broth, and the medium became a blue-green color (Figure1) pyocyanin pigment. According to (8), 250 ml of a *Pseudomonas aeruginosa* broth culture was collected after incubation, and the liquid was centrifuged at 5000 rpm for 15 min, supernatant and deposit were appeared, the supernatant was ignored. To extract the pyocyanin, chloroform has been added to deposit to yield pyocyanin. Extraction of chloroform led to the collection of the pyocyanin powder.



Figure (1): Pyocyanin pigment

Synthesis of cobalt and titanium (Co:TiO₂) core-shell nanoparticles

The first study This was the Preparation in the first stage to use pyocyanin for the Biosynthesis of cobalt (Co) nanoparticles, Method of synthesis is done by adding (5mg) of pyocyanin powder with (50ml) deionized distilled water DDW dispersed by ultrasonication bath for 30 minutes and dispersing (5g) of cobaltous chloride hexahydrate in 50 ml of pyocyanin Which was prepared in the past using in

a flask and shaking it overnight in a darkroom. The mixture was then centrifuged for 10 minutes at 5000 rpm. The precipitate of a solution containing the whole cobalt (Co) nanoparticles was twice washed with deionized distilled water to remove any remaining pyocyanin pigment. The precipitated nanoparticles were dried in an oven at 37°C overnight. Finally, the black powder was sealed in a dark container to prevent it from evaporating.(20) Preparing for the second stage used

pyocyanin for the biosynthesis of cobalt and titanium (Co:TiO₂) core-shell nanoparticles, the Process Cobalt nanoparticles Which were previously prepared were used to synthesize cobalt and titanium (Co:TiO₂) core-shell nanoparticles. The synthesis is carried out by dispersing 1.5 g of cobalt nanoparticles in 150 ml of pyocyanin Prepared (15mg) of pyocyanin powder with (150ml) deionized distilled water DDW dispersed by ultrasonication bath for 30min using a magnetic stirrer plate. Gradually drip 1 mL of titanium chloride into a flask and shake. The mixture was then centrifuged for 10

minutes at 5000 rpm. The precipitate of a solution containing the whole cobalt and titanium (Co:TiO₂) core-shell nanoparticles was twice washed with deionized distilled water to remove any remaining pyocyanin pigment. The precipitated nanoparticles were dried in an oven at 37°C overnight. Finally, the black powder was sealed in a dark container to prevent it from evaporating.

Results and discussion

VITEK 2 compact system (Figure 2) Illustrae result of *E. coli* Vitek.

bioMérieux Customer:		Microbiology Chart Report		Printed February 7, 2022 5:41:42 AM CST													
Patient Name: 121, .		Location:		Patient ID: hywer													
Lab ID: 109				Physician:													
Organism Quantity:		Selected Organism : <i>Escherichia coli</i>		Isolate Number: 1													
Source:				Collected:													
Comments:																	
Identification Information		Analysis Time: 4.12 hours		Status: Final													
Selected Organism		98% Probability		<i>Escherichia coli</i>													
ID Analysis Messages		Bionumber:		0405610570426611													
Biochemical Details																	
2	APPA	-	3	ADO	-	4	PyrA	-	5	IARL	-	7	dCEL	-	9	BGAL	+
10	H2S	-	11	BNAG	-	12	AGLTp	-	13	dGLU	+	14	GGT	-	15	OFF	+
17	BGLU	-	18	dMAL	+	19	dMAN	+	20	dMNE	+	21	BXYL	-	22	BAlap	-
23	ProA	-	26	LIP	-	27	PLE	-	29	TyrA	+	31	URE	-	32	dSOR	+
33	SAC	+	34	dTAG	+	35	dTRE	+	36	CIT	-	37	MNT	-	39	5KG	-
40	ILATk	-	41	AGLU	-	42	SUCT	+	43	NAGA	-	44	AGAL	+	45	PHOS	-
46	GlyA	-	47	ODC	+	48	LDC	+	53	IHISa	-	56	CMT	+	57	BGUR	+
58	O129R	+	59	GGAA	-	61	IMLTa	-	62	ELLM	+	64	ILATa	-			

Biochemical test

Table (3) and Figure (3) illustrate result biochemical test of *E.coli*

Table (3): The result of the biochemical test

No.	Test	Results
1	Oxidase test	-
2	Catalase test	+
3	Urase test	-
4	Indol test	+
5	Motility test	+
6	Simmons Citrate test	-
7	Methyl red test	+

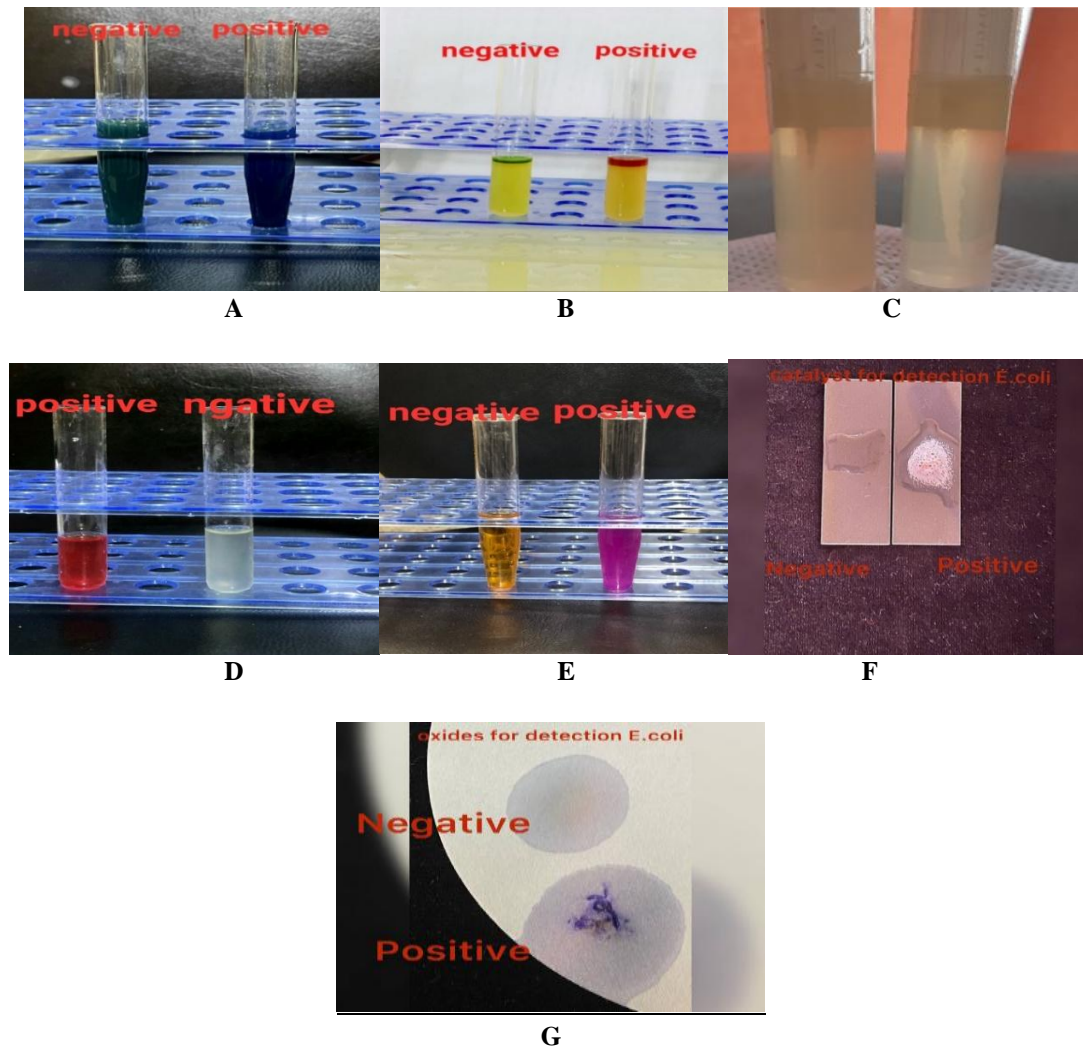


Figure (3): Biochemical tests for identification of bacterial isolate, (A): Simmons Citrate test, (B): Indole test, (C): Motility test, (D): Methyl Red test, (E): Urease test, (F): Catalase test, (G): Oxidase test.

Antibiotic susceptibility test of *E. coli*

Susceptibility to fifteen different antibiotics was examined using the disc diffusion technique suggested by the Clinical and Laboratory Standards Institute (CLSI, 2021) recommendations, and the findings given in (Figure4) shows variable degrees of resistance. antibiotic that were used for sensitive Antibiotics Aztreonam, Nitrofurantoin, Cefotaxime, Amoxicillin/Clavulanic acid, Trimethoprim Sulphamethoxazole,

Tobramycin, Piperacillin, Cefotaxime, Ertapenem and Gentamicin were shown to have the most significant rate of resistance in *E. coli* compared to the other bacteria studied. showed that Meropenem was the more effective antibiotic for Gram-negative bacteria. Medical scientists from Kathmandu University's School of Medicine determined that the antibiotic ampicillin had the lowest efficacy against *E. coli* meropenem, Ertapenem, and Levofloxacin were the most effective

antibiotics against *E. coli*. Many uropathogens, including multidrug resistant (MDR) Gram-negative bacteria and most organisms that generate-

lactamases, may be treated with this antibiotic (Figure 5) Statistical schedule Antibiotic Susceptibility Test of *E. coli* isolates.

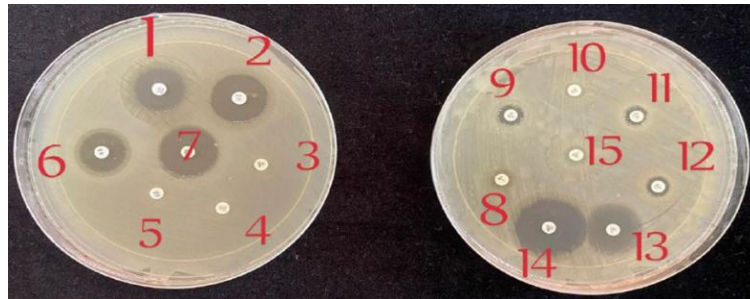


Figure (4): Antibiotic susceptibility test of *E. coli* isolates.

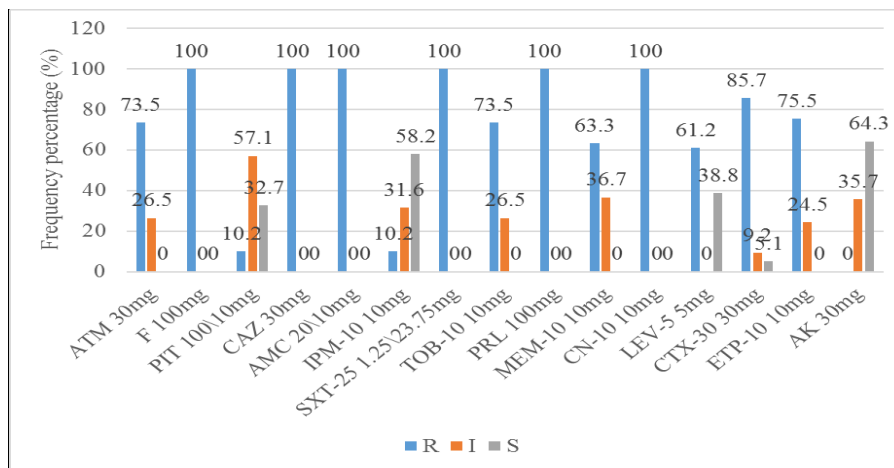


Figure (5): Statistical schedule antibiotic susceptibility test of *E. coli* isolates.

Result of biofilm test Congo red agar (CRA) method (Qualitative test)

To identify biofilm-forming bacteria, offer a qualitative approach employing Congo red agar (CRA) because of the color shift in colonies put on CRA media. *E. coli* isolates were

grown on CRA media for 24 hrs at 37C°, and the results reveal that the 98 isolates, 70% (68 isolates) with black colony crystals are biofilm makers, whereas 30% (30 isolates) with pink colony crystals are non-biofilm producers (Figure 6).

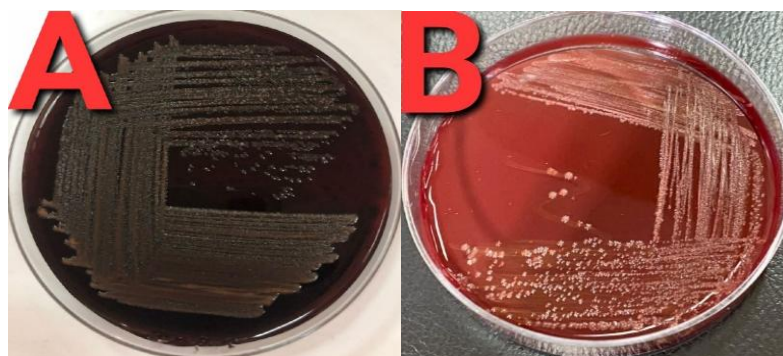


Figure (6): (A) *E. coli* biofilm formation, (B) *E. coli* non-biofilm producer.

Characterization of pyocyanin UV-VIS spectral analysis pyocyanin

The pyocyanin developed by *Pseudomonas aeruginosa* is characterized by scanning a UV-visible spectrophotometer (Figure 7) to detect

the maximum absorption, the result showed the absorbance of pyocyanin pigment at 315nm. the result showed the absorbance of pyocyanin pigment at 315nm and agree with (12).

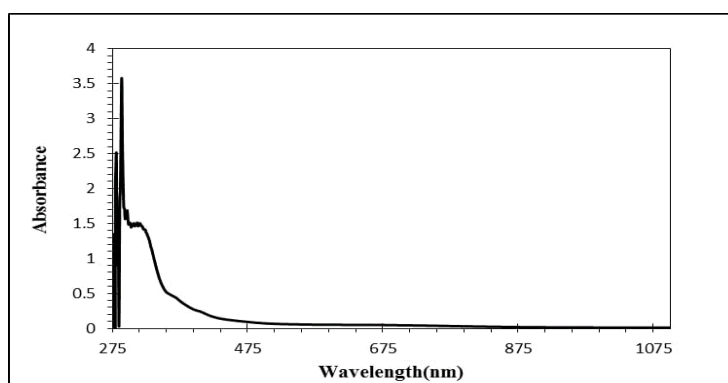


Figure (7): UV-VIS of pyocyanin

UV-VIS spectral analysis of cobalt and titanium (Co:TiO₂) core-shell nanoparticles

Is characterized by scanning a UV-visible spectrophotometer (Figure 8) to

detect the maximum absorption, the result showed the absorbance of Cobalt and titanium (Co:TiO₂) core-shell nanoparticles at 284 nm.

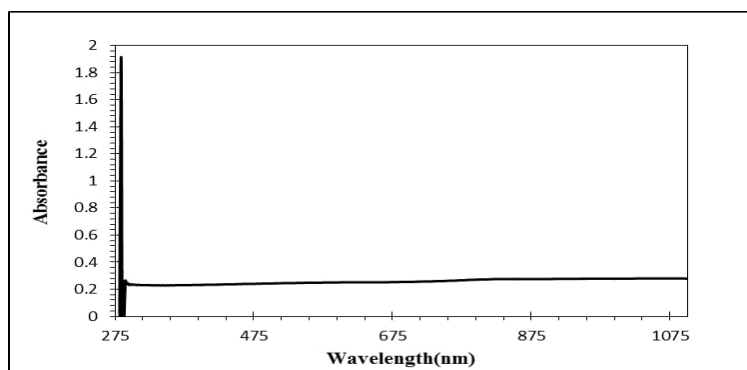


Figure (8): UV-VIS of cobalt and titanium (Co:TiO₂) core-shell nanoparticles.

Atomic force microscopy (AFM).

The surface shape formation of the (Co:TiO₂) NPs was studied by atomic force microscopy to show that (Co:TiO₂) NPs. (Figure 9). AFM

images show that the biosynthesized (Co:TiO₂) NPs are spherical. The size of an average diameter of 75.48 nm, (Table 4) was also measured by AFM.

Table (4): Average diameter of (Co: TiO₂) nanoparticle.

Sample	Average diameter(nm)	Roughness (nm)	R.M.S (nm)
Co-TiO ₂ NPs	75.48	10.8	13.6

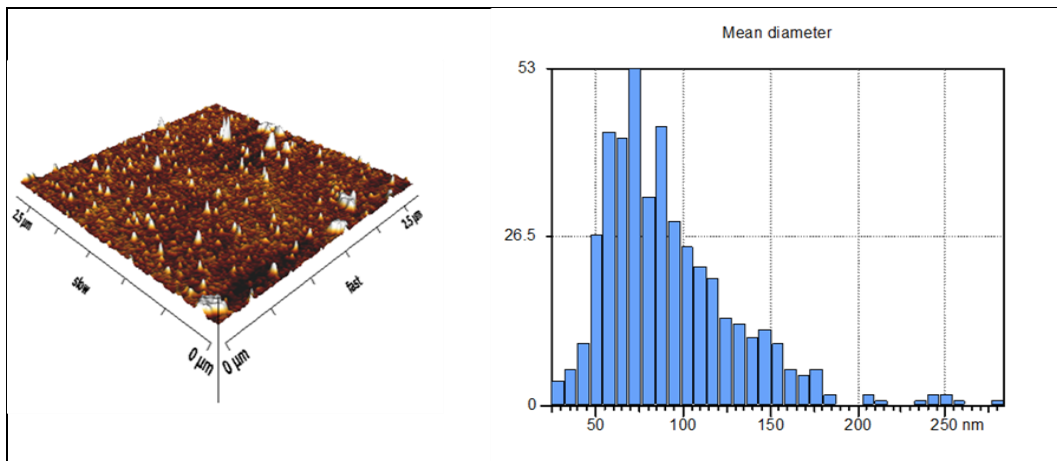


Figure (9): Atomic force microscopy (AFM) of (Co:TiO₂) nanoparticles synthesized using pyocyanin.

X-Ray diffractometer of (Co:TiO₂)

The purity and crystallinity of the as-synthesized (Co:TiO₂) nanoparticles were examined by using power X-ray diffraction (XRD), as shown in (Figure 10). its intrinsic components are comparable in XRD patterns to (Co:TiO₂) core-shell nanoparticles, (Co) nanoparticles have several orientations about the X-ray beam. Pattern XRD has been obtained over at $2\theta = 18.95^\circ, 36.8^\circ, 38.55^\circ, 45.95^\circ$ and 77.35° can be readily indexed as (111), (111), (222), (111) and (122). The XRD pattern shows that the samples are

single-phase and no other impurities distinct diffraction peak. the XRD pattern TiO₂ nanoparticles, XRD peaks located at $2\theta = 31.2^\circ, 33.95^\circ, 42.1^\circ, 54.55^\circ, 55.65^\circ, 59.3^\circ$ and 65.25° corresponding to (211), (102), (221), (511), (131), (142) and (123), Table (4-10). The XRD of (Co:TiO₂) core-shell nanoparticle. Planes respectively. Tropism of the particles at random and small particles caused the widening of diffraction rings made up of many diffraction spots, indicating that the nanoparticles are poly.

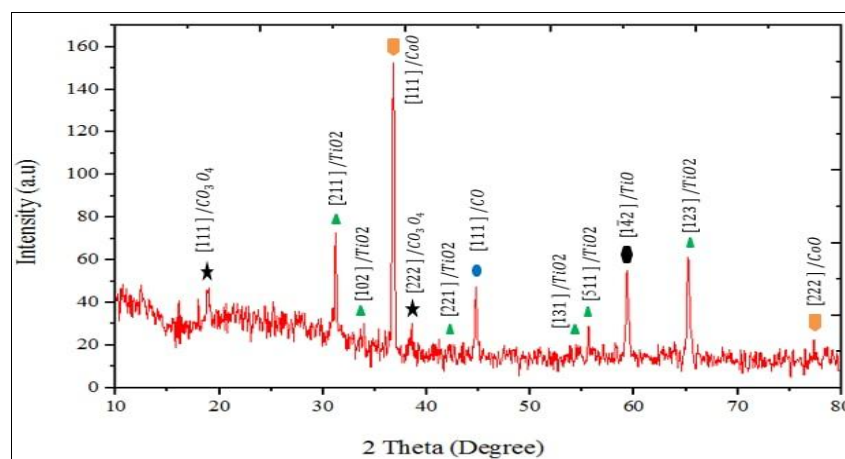


Figure (10) :The XRD images of (Co:TiO₂) core-shell nanoparticle.

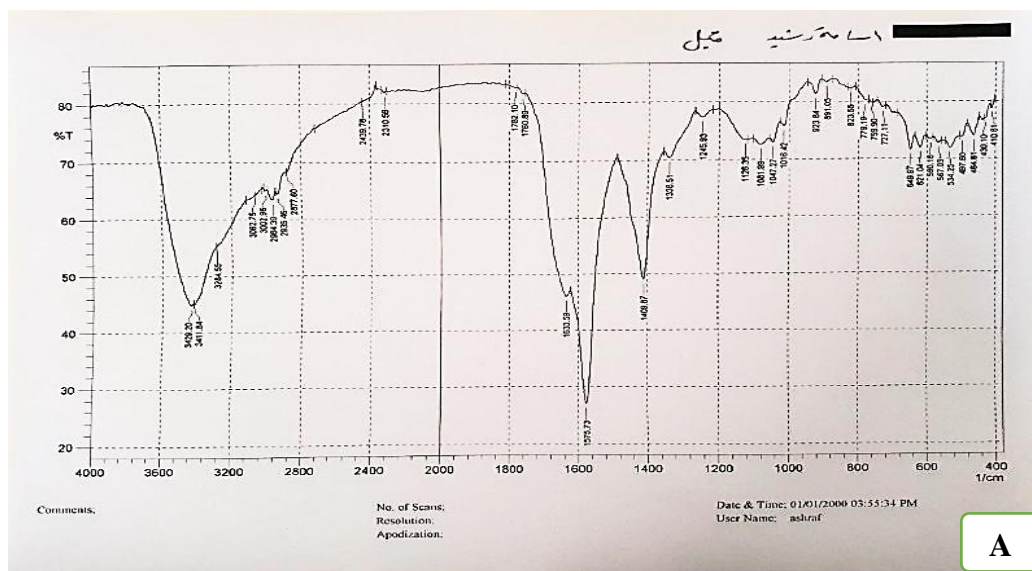
Fourier transform infrared (FTIR)

FTIR spectrum has determined the functional groups of nanoparticles. ((Figure11) Represents the absorption spectrum of Biologically synthesized nanoparticles in FTIR (Table 5) show the bands are observed around 3429.2-3411.8 cm^{-1} , corresponding to the

stretch movement of the hydroxyl group OH Alcohols and H bonds Phenols. The last is around at 1633.5cm^{-1} related to N-H bond Amines and the visible at $3434.9\text{-}3402.2\text{cm}^{-1}$ O=bond is due to the Oxide of metals it is due to aminescompndsou.

Table (5): FTIR of (Co:TiO₂) nanoparticle

	Frequency of Absorption(cm^{-1})	Bonds	Compound class of functional groups
Pyocyanin	3429.2-3411.8	O-H stretch	Alcohol and hydroxy compound
	3284.5	O-H stretch	Alcohol and hydroxy compound
	1633.5	C=C stretch	Alkenyl
	1575.7	N-H Bend	Amine
	1409.8	O-H Bend	Tertiary alcohol
	Pyocyanin +(Co:TiO₂)NPs	3433.0	N-H stretch
1631.6		N-H bend	Secondary amine
1577.6		N-H bend	Secondary amine
1441.8		C-H bend	Methyl
(Co:TiO₂) NPs	3434.9-3402.2	N-H stretch	Heterocyclic amine
	3259.4-3201.6	N-H stretch	Aromatic secondary
	1637.4	O-H stretch	Amine
	1577.6	N-H bend	Secondary amine
	1411.8	C-H bend	Methyl
	669.25	Metal Oxygen	Co,TiO ₂
	580.53	Metal Oxygen	Co,TiO ₂



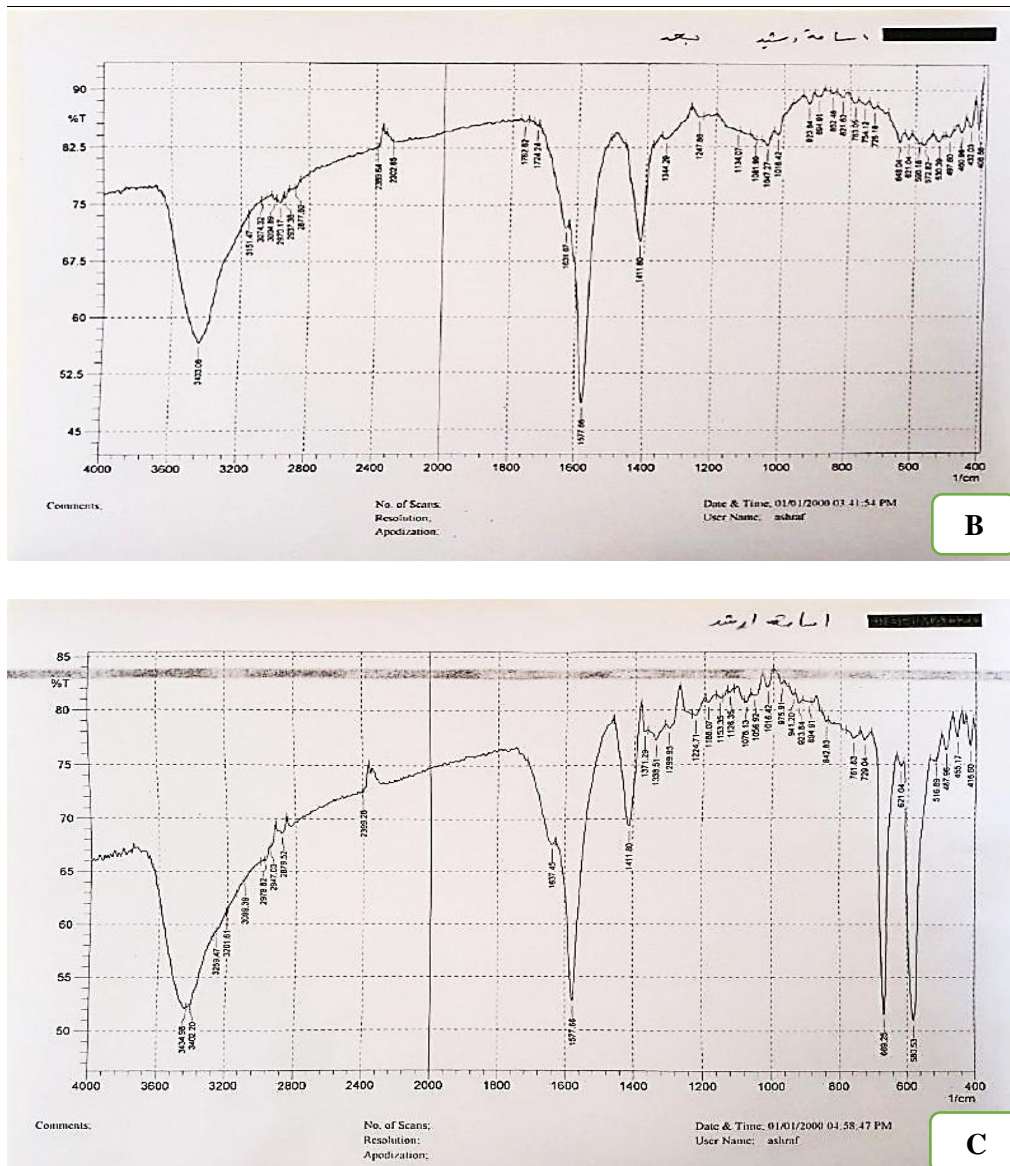


Figure (11): FTIR images of (Co:TiO₂) NPs synthesized using pyocyanin pigment, A: pyocyanin pigment. B: Pyocyanin pigment + (Co:TiO₂) NPs. C: (Co:TiO₂) NPs.

Field emission scanning electron microscope (FE-SEM) of cobalt and titanium (Co:TiO₂) core-shell nanoparticles

The FE-SEM images of (Co:TiO₂) nanoparticles showed that the structure of the particles is spherical; Small amounts of agglomerates were observed on the nanoparticle film surface due to decreased surface energy and magnetic properties, the presence of some significant size grains and the

aggregation of the NPs could be attributed to the increased surface areas and surface energies of the Co and TiO₂ core NPs. Because of the higher surface area to volume ratio, the nanoparticles were held together or agglomerated by the attractive physical forces between them. The FE- SEM analysis results in (Figures 12) revealed the morphology of the prepared (Co:TiO₂) nanoparticle, which was in good agreement with AFM results.

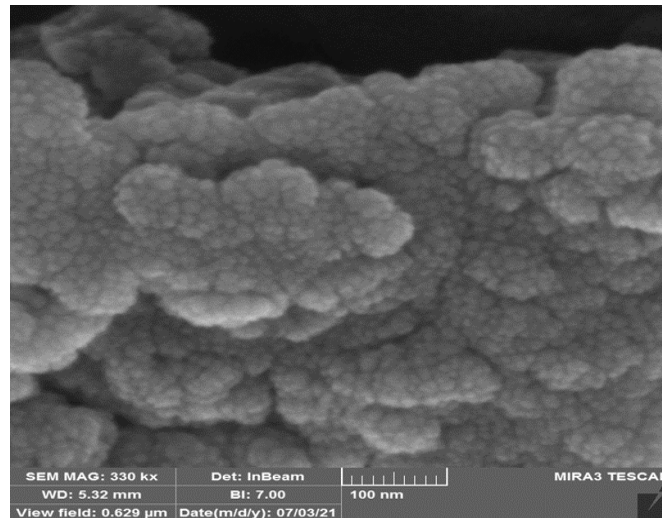


Figure (12): FE-SEM images of cobalt and titanium (Co:TiO₂) core-shell nanoparticles.

Transmission electron microscopy (TEM)

Such measures have been based on producing a large-intensity beam of electrons to be transmitted by samples to obtain the images and study the material micro-structuring with the atomic - molecule to assess. The resolution of very high spatial microstructure and morphology characteristics of nanoparticles generated. Subsequently, electrons will be targeted by an electromagnetic lens and pushed by thousands of volts, at much shorter rates than visible light.

Resulting in images on movies, digital cameras, or fluorescent screens. Even with a thinner sample, the observer will be seen through many atoms and seldom discover a single atom, additionally, the TEM analysis demonstrated that there were two different regions. The dark inner part represented the core, and the shiny part surrounding the dark region represented the shell, confirming the synthesis of (CO:TiO₂) core/shell nanoparticles. (Figure 13) TEM images of Cobalt and Titanium.

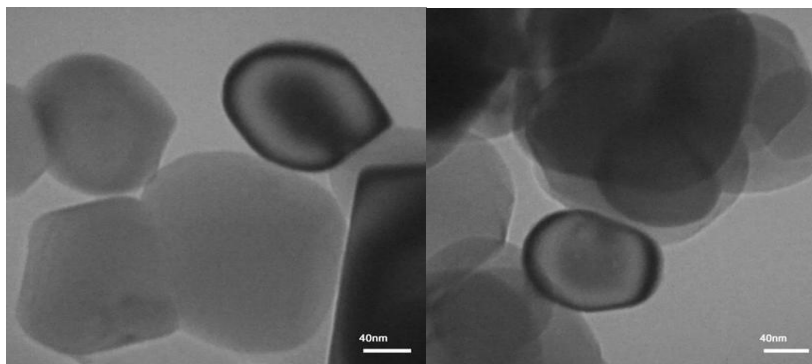


Figure (13): TEM images of Cobalt and Titanium (Co:TiO₂) core-shell nanoparticles.

Antibacterial activity of cobalt and titanium (Co:TiO₂) core-shell nanoparticles

The agar well diffusion method was

used to assess bacterial susceptibility to cobalt and titanium (Co :TiO₂) core-shell NPs. the Mueller Hinton medium was used in this test. *E. Coli* is

cultivated overnight at 37°C. After the incubation period, the standard inoculum for each bacterial isolate at a concentration of 1.5×10^8 CFU / mL was formed according to the standard solution of 0.5 McFarland. A sterile small swab has been dipped inside the tube containing the suspension and subsequently inoculated on the Muller Hinton agar (MH) plate to evenly cover bacteria on the plate surface. On MH agar plates, wells with a diameter of 6 mm were prepared aseptically and 1mL of different concentrations (200, 100, 50, 25, 12.5, 6.25, 3.125) $\mu\text{g/ml}$ of cobalt and titanium (Co:TiO₂) core-shell NPs were distributed into separate wells followed by overnight incubation at 37°C. Following incubation, the widths of the bacterial susceptibility zones were measured and reported. As a negative control, a well containing only

sterile distilled water was used.

Antibacterial susceptibility test

This is the first study to use (Co:TiO₂) core-shell nanoparticles as an antibacterial for MDR- *E. Coli* that have strong biofilm production. The results of using (Co:TiO₂) core-shell nanoparticles as antibacterial agents were found to be directly dependent upon the (Co:TiO₂) core-shell nanoparticles concentration. (Table6) show that the maximum inhibition zones of *E. Coli* were 37 mm at a concentration of 200 $\mu\text{g/ml}$ of (Co:TiO₂) core-shell nanoparticles, Whereas the minimum inhibition zones were located at 6.25 $\mu\text{g/ml}$ of (Co:TiO₂) core-shell nanoparticles concentrations, the inhibition zone depended on the concentration of (Co:TiO₂) core-shell nanoparticles. see (Figure14).

Table (6): The inhibition zone of antibacterial effect of (Co:TiO₂) NPS on *E. Coli*

No.	(Co:TiO ₂)NPScon.($\mu\text{g/ml}$)	ZONE OF Diameter (mm)
1	200	37
2	100	34
3	50	29
4	25	27
5	12.5	20
6	6.25	17
7	3.125	No inhibition Zone

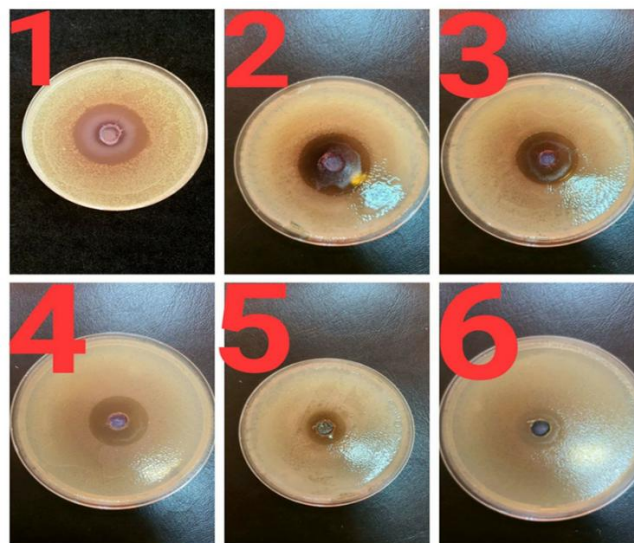


Figure (14): Antibacterial activity of (Co:TiO₂) NPS on *E. Coli*.

Inhibition of the biofilm formed of (MDR) *E. Coli* by synthesized (Co:TiO₂) nanoparticles

E. Coli biofilm formation for strong biofilm producers was measured in response to sub-MICs of (Co:TiO₂) core-shell nanoparticles (100, 50, 25, 12.5, 6.25, and 3.125 µg/ml) by using tissue culture plates and crystal violet staining method, as shown in (Figure 15) and. Biosynthesized (Co:TiO₂) core-shell nanoparticles showed considerable inhibition in the biofilm formation. Along with an increase in dilution of sub-MICs, biofilm-forming inhibition decreased significantly. As shown in

(Figure 15) and (Table 7), (Co:TiO₂) core-shell nanoparticles can suppress biofilm formation by reducing bacterial adhesion. When bacteria in a biofilm are exposed to (Co:TiO₂) core-shell nanoparticles, they are destroyed; (Co:TiO₂) core-shell nanoparticles exhibited antibiofilm action, making an attractive material for usage in various applications to global health issues caused by the rise of resistant microbes. (21) It is the first study about the effect of biosynthesis (Co:TiO₂) nanoparticles against biofilm *E. Coli*.

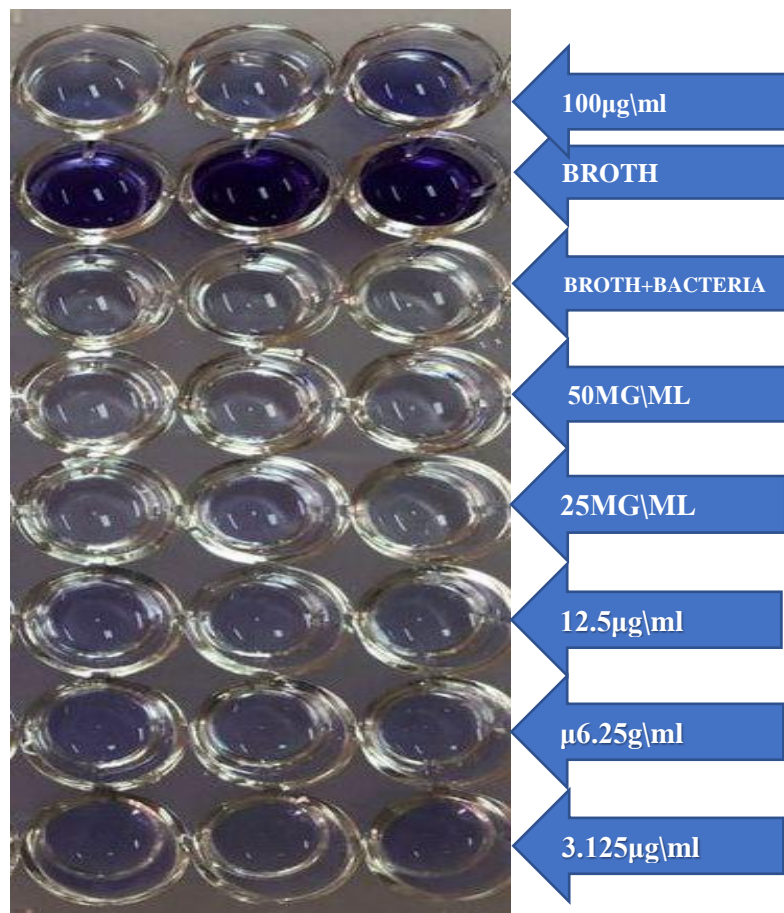


Figure (15): Inhibition of *E. Coli* biofilm using (Co:TiO₂) nanoparticles.

Table (7): The effect of biosynthesized (Co:TiO₂) NPs on MDR *E. Coli* biofilm

Groups	Mean ± SE	
Broth	0.06 ± 0.002	D
Bacteria	1.03 ± 0.12	A
MIC1 (0.1)	0.13 ± 0.01	C
MIC2 (0.05)	0.12 ± 0.006	C
MIC3 (0.025)	1.07 ± 0.22	A
MIC4 (0.012)	1.01 ± 0.08	A
MIC5 (0.006)	0.97 ± 0.08	AB
MIC6 (0.003)	0.71 ± 0.06	B
Duncan test: the similar letters referred to a non-significant difference		

References

- Altaee, M. F.; Yaaqoob, L. A. and Kamona, Z. K. (2020). Evaluation of the Biological Activity of Nickel Oxide Nanoparticles as Antibacterial and Anticancer Agents. *Iraqi Journal of Science*, 61(11): 2888-2896.
- Awati, P.S.; Awate; S.V.; Shah, P.P. and Ramaswamy; V. (2003). Photocatalytic decomposition of methylene blue using nanocrystalline anatase titania prepared by ultrasonic technique. *Catalysis Communications*, 4(8): 393-400.
- Bunaciu, A. A.; UdriȘTioiu, E. G. and Aboul-Enein, H. Y. (2015). X-ray diffraction: instrumentation and applications. *Critical Reviews in Analytical Chemistry*, 45(4): 289-299.
- Djordjevic, D.; Wiedmann, M. and McLandsborough, L. A. (2002). Microtiter Plate Assay for Assessment of *Listeria monocytogenes* Biofilm Formation. *Applied and Environmental Microbiology*, 68(6): 2950-2958.
- Gault, N.; Sandre, C.; Poncy, J. L.; Moulin, C.; Lefaix, J. L. and Bresson, C. (2010). Cobalt toxicity: chemical and radiological combined effects on HaCaT keratinocyte cell line. *Toxicology in vitro : an international journal published in association with BIBRA*, 24(1): 92-98.
- Hamid, O. S. and Mahmood, S. S. (2021). the synergistic effect of gold nanoparticle loaded with ceftazidime antibiotic against multidrug resistance *Pseudomonas aeruginosa*. *The Iraqi Journal of Agricultural Science*, 52(4): 828-835.
- Hamza, M. R. and Yaaqoob, L. A. (2020). Evaluation the Effect of Green Synthesis Titanium Dioxide Nanoparticles on *Acinetobacter Baumannii* Isolates. *The Iraqi Journal of Agricultural Science*, 51(6): 1486-1495.
- Jayaseelan, S.; Ramaswamy, D. and Dharmaraj, S. (2014). Pyocyanin: production, applications, challenges and new insights. *World Journal of Microbiology and Biotechnology*, 30(4): 1159-1168.
- Kavitha, K. S.; Baker; S.; Rakshith, D.; Kavitha, H. U.; Yashwantha Rao, H. C.; Harini, B. P., *et al.* (2013). Plants as green source towards synthesis of nanoparticles. *International Research Journal of Biological Sciences*, 2(6): 66-76.
- Khan, S.; Ansari, A. A.; Khan, A. A.; Ahmad, R.; Al-Obaid, O. and Al-Kattan, W. (2015). In vitro evaluation of anticancer and antibacterial activities of cobalt oxide nanoparticles. *Journal of Biological Inorganic Chemistry*. 20(8): 1319-1326.
- Muhaidi, M.J.; Aziz, L.M. and Ahmed, M.N. (2018). Genetic evaluation of phenazine synthesized by *Pseudomonas aeruginosa* isolated genital tract of farm animals. *Iraqi Journal of Agricultural Sciences*, 49(2): 151-157.
- Nawas, T. (2018). Extraction and purification of pyocyanin: a simpler and more reliable method. *MOJ Toxicology*, 4(6):1102-1406.
- Ranquet, C.; Ollagnier-de-Choudens, S.; Loiseau, L.; Barras; F. and Fontecave; M. (2007). Cobalt stress in *Escherichia coli*: the effect on the iron-sulfur proteins. *Journal of Biological Chemistry*, 282(42): 30442-30451.
- Schulze, A.; Mitterer, F.; Pombo, J. P. and Schild, S. (2021). Biofilms by bacterial human pathogens: Clinical relevance - development, composition and regulation - therapeutical strategies. *Microbial cell (Graz, Austria)*, 8(2): 28-56.
- Sharma, G.; Sharma, S.; Sharma, P.;

- Chandola, D.; Dang, S.; Gupta, S., *et al.* (2016). *Escherichia coli* biofilm: development and therapeutic strategies. *Journal of Applied Microbiology*, 121(2): 309–319.
16. Sood, U.; Singh, D. N.; Hira, P.; Lee, J. K.; Kalia, V. C.; Lal, R., *et al.* (2020). Rapid and solitary production of mono-rhamnolipid biosurfactant and biofilm inhibiting pyocyanin by a taxonomic outlier *Pseudomonas aeruginosa* strain CR1. *Journal of Biotechnology*, 307: 98-106.
 17. Tran, T. H.; Nosaka, A. Y. and Nosaka, Y. (2006). Adsorption and photocatalytic decomposition of amino acids in TiO₂ photocatalytic systems. *The Journal of Physical Chemistry. B*, 110(50): 25525-25531.
 18. Velayutham, K.; Rahuman, A. A.; Rajakumar, G.; Santhoshkumar, T.; Marimuthu, S.; Jayaseelan, C., *et al.* (2012). Evaluation of *Catharanthus roseus* leaf extract-mediated biosynthesis of titanium dioxide nanoparticles against *Hippobosca maculata* and *Bovicola ovis*. *Parasitology Research*, 111(6): 2329-2337.
 19. Wu, J.; Bai, G.; Eastman, J.A.; Zhou, G. and Vasudevan, V. K. (2005). Synthesis of TiO₂ Nanoparticles Using Chemical Vapor Condensation. *Materials Research Society*, 879, Z7.12.1.
 20. Yaaqoob, L. A. (2022). Evaluation of the Biological Effect Synthesized Iron Oxide Nanoparticles on *Enterococcus Faecalis*. *Iraqi Journal of Agricultural Sciences*, 53(2): 440-452.
 21. Al-Ahmer, S. D., Shami, A. M., & AL-Saadi, B. Q. H. (2018). Using of Hybrid Nanoantibiotics as Promising Antimicrobial Agent. *Iraqi Journal of Biotechnology*, 17(3).